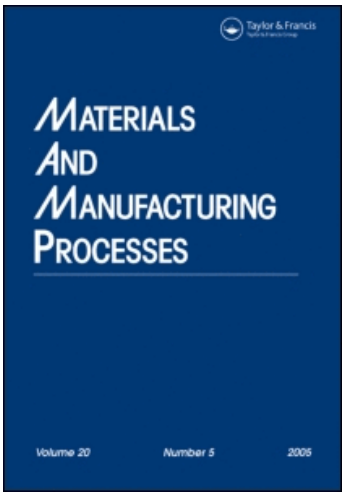

Materials and Manufacturing Processes
Publication details, including instructions for authors and subscription information:
http://www.informaworld.com/smpp/title~content=t713597284

Neural Network Modeling and Particle Swarm Optimization (PSO) of Process Parameters in Pulsed Laser Micromachining of Hardened AISI H13 Steel

J. Ciurana [a]; G. Arias [b]; T. Ozel [c]
[a] Department of Mechanical Engineering and Industrial Construction, Universitat de Girona, Spain [b] Department of Mechanical Engineering, Universitat Politècnica de Catalunya, Spain [c] Department of Industrial and Systems Engineering, Rutgers University, New Jersey, USA

Online Publication Date: 01 March 2009

To cite this Article Ciurana, J., Arias, G. and Ozel, T.(2009)'Neural Network Modeling and Particle Swarm Optimization (PSO) of Process Parameters in Pulsed Laser Micromachining of Hardened AISI H13 Steel',Materials and Manufacturing Processes,24:3,358 — 368

To link to this Article: DOI: 10.1080/10426910802679568

URL: http://dx.doi.org/10.1080/10426910802679568

Materials and Manufacturing Processes, 24: 358–368, 2009

ISSN: 1042-6914 print/1532-2475 online
DOI: 10.1080/10426910802679568

Taylor & Francis
Taylor & Francis Group

Neural Network Modeling and Particle Swarm Optimization (PSO) of Process Parameters in Pulsed Laser Micromachining of Hardened AISI H13 Steel

J. Ciurana[1], G. Arias[2], and T. Ozel[3]

[1]*Department of Mechanical Engineering and Industrial Construction, Universitat de Girona, Spain*
[2]*Department of Mechanical Engineering, Universitat Politècnica de Catalunya, Spain*
[3]*Department of Industrial and Systems Engineering, Rutgers University, New Jersey, USA*

This article focuses on modeling and optimizing process parameters in pulsed laser micromachining. Use of continuous wave or pulsed lasers to perform micromachining of 3-D geometrical features on difficult-to-cut metals is a feasible option due the advantages offered such as tool-free and high precision material removal over conventional machining processes. Despite these advantages, pulsed laser micromachining is complex, highly dependent upon material absorption reflectivity, and ablation characteristics. Selection of process operational parameters is highly critical for successful laser micromachining. A set of designed experiments is carried out in a pulsed Nd:YAG laser system using AISI H13 hardened tool steel as work material. Several T-shaped deep features with straight and tapered walls have been machining as representative mold cavities on the hardened tool steel. The relation between process parameters and quality characteristics has been modeled with artificial neural networks (ANN). Predictions with ANNs have been compared with experimental work. Multiobjective particle swarm optimization (PSO) of process parameters for minimum surface roughness and minimum volume error is carried out. This result shows that proposed models and swarm optimization approach are suitable to identify optimum process settings.

Keywords Laser technology; Mold making; Neural network models; Surface roughness.

1. Introduction

Nowadays, lasers are increasingly used in numerous industries to produce high precision products by means of cutting, welding, marking, etc. Recently, the laser machining (or milling) technology is increasing its presence in production systems due to technological improvements in laser machines. Laser machining of metals has become a feasible and reliable technology for manufacturing and industrial production. Today, laser machining is considered as a good alternative to mechanical cutting due to its ability and flexibility to process several quantities of difficult-to-cut metal parts and geometrical features with minimum amount of waste. The advantage of laser machining is that the process does not need tools, special fixtures or jigs for the workpiece because it is a noncontact operation [1]. Compared with other conventional mechanical processes, laser machining (milling) removes much less material, involves highly localized heat input to the workpiece, minimizes distortion, and offers no tool wear. It does not need replaceable or expensive tools and does not produce mechanical forces that can damage workpieces [2].

Laser machining process is suitable for stainless steel and other alloy steels that are used in die and mould inserts, and achieves high accuracy with good productivity [3–5]. It produces geometrical features often desired in die and mould inserts, and allows producing small and complex grooves and cavities with high precision. Laser machining (milling) shapes a workpiece into a well-defined geometrical feature that are typically very difficult to produce with mechanical end milling such as straight/curved grooves, angled channels with straight walls, and rectangular pockets with sharp corners, especially in a length scale measured in millimeters to micrometers.

Pulsed laser micromachining operates as a sequential ablation process causing material vaporization, and, as a result of this iteration, the geometrical feature is machined. It offers, among others, the following advantages: deep penetration, narrow heat affected zones, and reduced tendency to spatter, incomplete fusion, and root bead porosity [1]. Laser-workpiece material interaction is influenced by many process parameters and considered highly nonlinear. There are a number of operational parameters which must be set when manufacturing process is done. Considering the laser equipment those parameters are: laser power, wavelength, efficiency, and emerging beam diameter. On the delivery optics the parameters are focused beam diameter, fiber diameter (in case of optical fiber delivery), focal length of the focusing lens, focus depth, and amount of power loss in the delivery optics and fiber. All those parameters are specified by the desired penetration depth so the operator cannot manipulate them. Furthermore, the remaining parameters are concerning the operation such as cutting and scanning speeds, focus position related to the upper material surface, nozzle tip diameter, distance between the tip and the material (stand-off distance), assistant gas type, and assistant gas pressure [4–6]. In case of pulsed lasers, pulse frequency, pulse duration, and peak power should be also considered as additional parameters. These operation parameters are variable and can be adjusted

Received June 26, 2008; Accepted September 25, 2008
Address correspondence to T. Ozel, Department of Industrial and Systems Engineering, Rutgers University, Piscataway, NJ 08854, USA; E-mail: ozel@rutgers.edu

in areas to optimize the desired quality of the machined features.

There have been many studies aimed at systematically investigating the influence of process variables during pulsed Nd:YAG laser machining [4–9]. Considering all those operational parameters, it is highly difficult to model the influence of them on resultant workpiece geometry and surface quality using conventional methods. Usually, the operator selects them based on experience or designs appropriate experiments to determine somewhat reasonable parameter combination for the desired results. But, this trial-and-error approach is high costly in time and labor. Especially when a prototyping batch is carried out and due to the short lead time constraints, the results cannot be fully optimized.

There are several research works which mainly deal with how process parameters affect the quality of the resultant surfaces or geometrical features using experimental and statistical analysis tools [10–13]. Some researchers implemented soft-computing tools such as neural networks to represent the effects of process parameters on the outcomes of the laser machining [14, 15]. Despite all of these studies, it is still not well-understood how laser milling performs machining complex 3-D features such as grooves, channels, pockets, especially how to utilize laser micromachining when the features become microfeatures.

The work presented in this article provides the needed insight for improving the laser milling as a micromanufacturing process. As a result, an artificial neural network (ANN) model of the micromachining process has developed in order to find more satisfactory process parameters for a particular machining set-up. It is highly useful to capture the influence of laser process parameters such as pulse intensity, scanning speed and pulse frequency on desired dimensions, and surface roughness and develop a predictive system which identifies the optimum set of process parameters. Considering all laser process parameters, it is important to identify which ones have more effect on resultant feature quality, and in what degree changing these process parameters will affect the feature quality. Therefore, this work will contribute to the understanding the relations between process parameters (pulse characteristics, speed, and laser intensity) and quality of the geometrical features on the final products. The work also deals with modelling the relations between process parameters and dimensional quality and surface roughness of the features produced by using ANN. The ANN model also enables better process design, reduces the use of trial-and-error methods, eliminates the need for frequent experimental trials, and minimizes the need for post-machining operations due to improved quality.

2. Experimental procedure and neural network modeling

In this section, the experimental procedure and the results will be discussed. In addition, the use of soft computing methods such as neural network modeling and particle swarm optimization (PSO) are explained.

2.1. Experimental Procedure

The main objective of this experimental work was to investigate the influence of laser process parameters on dimensional precision and surface quality in laser micromachining of hardened AISI H13 tool steel which is a popular material for die and mould inserts. The experiments were performed using Deckel Maho Lasertec 40 machine, Nd:YAG lamp pumped solid-state laser, 100 W/0.134 hp average laser power, 1,064 nm wave length with a laser beam spot diameter 0.03 mm. In the experiments, the following process parameters were used: pulse intensity (*PI*) 50, 75, and 100%, scanning speed (*SS*) of 225, 375, and 525 mm/s and pulse frequency (*PF*) of 60, 80, and 100 Hz.

In laser micromachining the laser beam machines directly to the material to be removed by creating a high temperature which generates the ablation of the material, and, consequently, the material was removed. Figure 1 shows how laser beam move in rotation to operate perpendicular. In that set-up the machine works with four axes, which allows operating laser beam directly perpendicular to surface to be machined. This operating mode permits to obtain several geometrical angle groove features; however, when the mirror is moving, the focal distance is not always exactly the same so then energy used to machine is not constant. The material was removed layer by layer in the depth direction. The machine table where the part is fixed moves in X direction meantime laser beam is moving by rotation through the mirrors movement. This combination of movements composes the volume which has been removed.

AISI H13 hardened tool steel was used as a part test. This material was selected because it is commonly used when moulds inserts are needed. The part was machined to obtain 3-D groove features as shown in Fig. 2. This test part combines several geometrical and dimensional characteristics and minimizes the volume to be removed that helps experiments do not carry long time. Measurable dimensions on test part are also indicated in Fig. 2. The desired dimensions are angles $A = 135$ degrees, $B = 135$ degrees, $C = 2$ mm, $D = 1$ mm. Furthermore, the surface roughness was measured as an indication of surface quality. The dimensional measurements were performed by 4× magnification lens attached to a ColorView™ high definition camera supported by PerfectImage™ software. The values were extracted and recorded throughout by using the side view of test part. The measurement of surface roughness parameter R_a on finish bottom surface, was made by a stylus instrument, with a cut off of 0.8 mm, in accordance to ISO/DIS 4287/1E, on a Mitutoyo SV2000 Surftest equipment.

2.1.1. Experimental Design. A three factor-three level factorial design was used to determine the effects of pulse intensity, scanning speed, and pulse frequency on resultant dimensional precision and surface roughness in microlaser machining of H13 hardened tool steel. The factors and factor levels are summarized in Table 1. These factor levels results in a total of 27 unique factor level combinations. The response variables are the work piece surface roughness, R_a [μm], angular dimensions, A and B

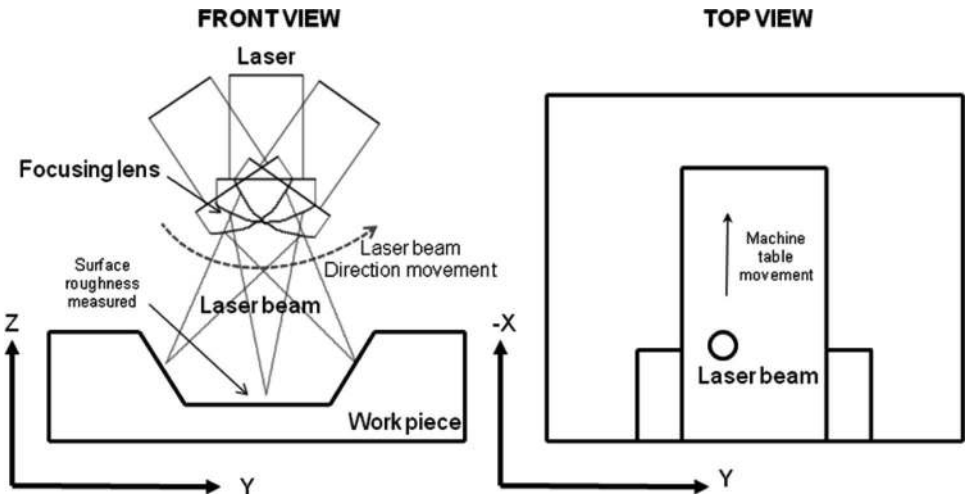

FIGURE 1.—Illustration of the laser micromachining (milling) process.

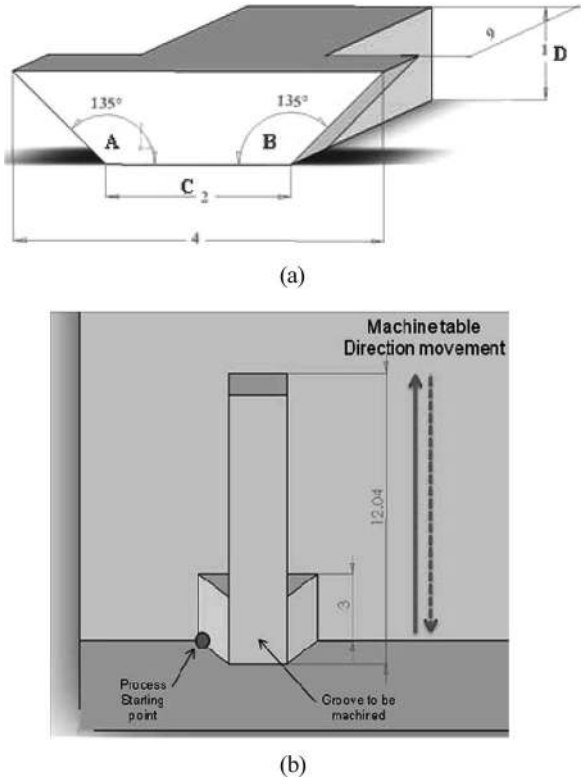

FIGURE 2.—(a) Desired material removal volume with dimensions in mm; (b) Geometry of the groove to be machined.

[degrees], linear width dimension, C [mm], linear depth dimension D [mm] as indicated in Fig. 2, and process time [min]. The experimental results obtained are given in Table 2. In addition with all these values given in Table 2, the actual volume of material removed is also calculated. Considering that target volume should be 27 mm^3, volume error can be obtained comparing actual volume removed with the target volume, as shown in Eq. (1). At last, material removal rate (MRR) parameter can be obtained dividing by process time according Eq. (2).

TABLE 1.—Factor and factor levels.

Factors	Factor levels
Pulse intensity (*PI*)	50, 75, 100 [%]
Scanning speed (*SS*)	225, 375, 525 [mm/s]
Pulse frequency (*PF*)	60, 80, 100 [Hz]

$$\varepsilon_{\text{vol}} = \text{Actual Volume Removed} - \text{Target Volume} \quad (1)$$

$$\text{MRR} = \text{Actual Volume Removed/Machining Time.} \quad (2)$$

2.2. Neural Network Modeling

Neural networks are nonlinear mapping systems consisting of neurons and weighted connection links, which consist of user-defined inputs and produce an output that reflects the information stored in connections during training. In this study, a multilayer neural network consisting of three layers, i.e., input, hidden, and output layer, was considered. We have tested several backpropagation training algorithms, including *gradient descent* with momentum and adaptive learning method, *resilient backpropagation* algorithm, and the *Levenberg–Marquardt* algorithm. In addition, the *Levenberg–Marquardt* with *Bayesian regularization* is used to improve the generalization capability of the neural networks [16].

In all of those neural network models, the nonlinear *tanh* activation functions are used in the hidden layer, and input data are normalized in the range of $[-1, 1]$. Linear activation functions are used in the output layer. The weights and biases of the network are initialized to small random values to avoid immediate saturation in the activation functions. The data set is divided into two sets as training and test sets. Neural networks are trained by using training data set, and their generalization capacity is examined by using test sets. The training data were never used in test data. Matlab's neural network toolbox is used

TABLE 2.—Experimental results.

Trial	Pulse intensity [%]	Scanning speed [mm/s]	Pulse frequency [Hz]	Angle A [degrees]	Angle B [degrees]	Width C [mm]	Depth D [mm]	Surface finish R_a [μm]	Machining time [min]	Volume error [mm^3]	Actual MRR [mm^3/s]
1	50	225	60	147.270	149.980	2.130	0.805	2.323	118	2.456	0.208
2	50	225	80	164.335	165.830	2.140	0.385	3.480	118	12.767	0.121
3	50	225	100	170.238	170.238	2.140	0.170	0.844	118	19.670	0.062
4	50	375	60	161.885	162.060	2.160	0.375	1.930	75	13.823	0.176
5	50	375	80	171.410	171.410	2.145	0.140	1.848	75	20.616	0.085
6	50	375	100	154.385	156.345	2.165	0.315	0.357	75	16.752	0.137
7	50	525	60	167.770	166.430	2.160	0.210	1.630	57	18.799	0.144
8	50	525	80	174.136	174.136	2.150	0.095	0.831	57	21.774	0.092
9	50	525	100	177.207	177.207	2.155	0.045	0.323	57	23.069	0.069
10	75	225	60	125.045	125.230	2.125	1.690	2.142	118	−19.663	0.395
11	75	225	80	128.575	128.990	2.175	1.615	2.358	118	−19.045	0.390
12	75	225	100	135.165	136.150	2.165	1.370	3.523	118	−12.799	0.337
13	75	375	60	134.790	134.860	2.130	1.390	1.762	75	−12.673	0.529
14	75	375	80	134.845	136.050	2.195	1.335	1.887	75	−12.233	0.523
15	75	375	100	150.560	148.370	2.130	0.610	2.095	75	8.302	0.249
16	75	525	60	143.230	140.555	2.005	0.950	1.057	57	0.504	0.465
17	75	525	80	144.685	143.435	2.090	0.885	1.013	57	1.141	0.454
18	75	525	100	151.595	154.995	2.070	0.405	2.618	57	14.514	0.219
19	100	225	60	118.815	120.305	2.120	1.960	2.072	118	−26.198	0.451
20	100	225	80	120.640	120.985	2.135	1.840	2.282	118	−23.433	0.427
21	100	225	100	123.420	124.945	2.140	1.690	4.375	118	−19.843	0.397
22	100	375	60	124.550	125.145	2.140	1.685	1.485	75	−19.790	0.624
23	100	375	80	123.860	127.235	2.275	1.685	1.674	75	−22.617	0.662
24	100	375	100	126.665	128.725	2.190	1.585	1.776	75	−18.330	0.604
25	100	525	60	129.760	129.045	2.100	1.480	2.615	57	−13.944	0.718
26	100	525	80	131.010	129.785	2.075	1.520	1.575	57	−14.729	0.732
27	100	525	100	128.440	128.950	2.060	1.465	1.839	57	−12.735	0.697

to train neural networks. Simulations with test data repeated many times with different weight and bias initializations.

2.2.1. Prediction of Surface Roughness, Dimensional Accuracy, and MRR. Surface roughness (R_a), geometrical and dimensional features (A, B, C, D), error in volume removed (ε_{vol}), and MRR are predicted with a trained feed-forward neural network as shown in Fig. 3. Pulse intensity (*PI*), cutting speed (*SS*), pulse frequency (*PF*), and time are used as inputs to neural network. These neural networks are trained with 18 data sets (laser micromachining conditions) without including 9 data sets as given in Table 2. They are tested on 9 data sets which are not used in training. Training algorithms and network architectures are selected for minimum root-mean-squared (*rms*) error for best predictions using a training procedure. Selection process for the ANN architecture includes identifying first most optimum training algorithm and most optimum number of hidden layer neurons for a minimized *rms* error. Hence, the number of neurons in the hidden layer is decided by choosing the network structure that minimizes the *rms* error with trial-and-error. The results of these tests are summarized in Table 3.

The *resilient backpropagation* algorithm is found most optimum for training neural networks and network structures of 4-5-1, 4-4-1, and 4-4-1 are found sufficient for neural networks designed for predicting surface roughness, R_a, Angle A, and Angle B, respectively. On the other hand, the *Levenberg–Marquardt* algorithm has performed better

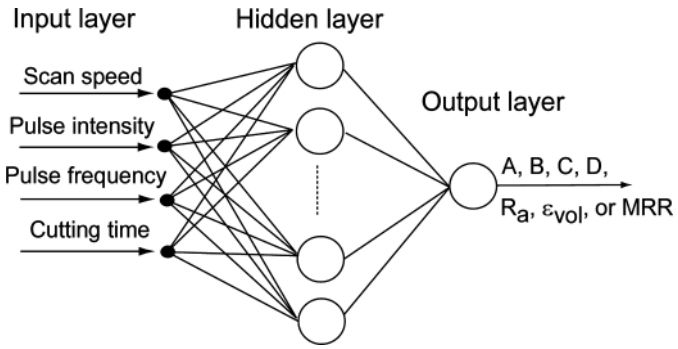

FIGURE 3.—Architecture of multilayer feed-forward neural network used for predictions.

TABLE 3.—Selection of ANN architecture and backpropagation training algorithms.

Output	Network structure	rms error Gradient descent w/momentum & adaptive learning	rms error Resilient back-propagation	rms error Levenberg–Marquart	rms error Bayesian regularization
R_a	4-5-1	12.4915	2.1175	7.2351	27.1388
A	4-4-1	0.6296	0.4354	1.5421	1.9446
B	4-4-1	0.9448	0.4536	0.7029	1.4334
C	4-4-1	0.4512	0.4103	0.2735	2.3599
D	4-5-1	1.9654	0.6894	0.1279	8.1878
ε_{vol}	4-5-1	85.3276	27.3398	0.1931	54.0504
MRR	4-5-1	1.9044	1.2828	0.3020	6.3671

for training neural networks. Network structures of 4-4-1 for predicting Width C and 4-5-1 for predicting Depth D, volume error, and actual MRR are found to be sufficient. This approach decreased the size of each neural network thus enabled faster convergence and better predictions of output values as explained in [17, 18]. Predictions using these neural networks are given in Section 3.1.

2.3. PSO

In this study, PSO as an evolutionary computation (EC) method inspired by flocking birds is utilized. This population-based stochastic optimization technique developed [19] and applied to many different systems including machining [20].

PSO is initialized with a population of random solutions, and this initial population evolves over generations to find optima. However, in PSO, each particle in population has a velocity, which enables them to fly through the problem space instead of dying and mutations. Therefore, each particle is represented by a position and a velocity. Modification of the position of a particle is performed by using its previous position information and its current velocity. Each particle knows its best position (personal best) so far and the best position achieved in the group (group best) among all personal bests. These principles can be formulated as:

$$v_i^{k+1} = wv_i^k + c_1 rand_1(pbest_i - x_i^k) + c_2 rand_2(gbest_i - x_i^k), \quad (3)$$

where

v_i^k: velocity of agent i at iteration k
x_i^k: current position of agent i at iteration k
$pbest_i$: personal best of agent i
$gbest$: best position in the neighborhood
$rand$: random number between 0 and 1
w: weighting function
c_j: learning rate $j = 1, 2$

$$x_i^{k+1} = x_i^k + v_i^{k+1}. \quad (4)$$

The first term on the right-hand side of Eq. (3) is the previous velocity of the particle. Weighting function w is set at a large value at the beginning of the search and decreased to a smaller value over the iterations to confine the search in a smaller region in later iterations, or it could be selected randomly. The second and third terms are used to change the velocity of the particle according to *pbest* and *gbest* values. The random numbers used in the velocity update step give the PSO a stochastic behavior. The iterative approach of PSO can be described as follows:

Step 1: First, a population size is specified. Initial positions and velocities of agents are generated randomly. Then, objective function values for each agent (or particle) are calculated. For the first iteration, *pbest* is set as the current position of each particle. The *pbest* with best objective function value among the agents is set as *gbest* and this value is stored.

Step 2: In the next iteration, the new position of the agents (particles) in the solution space is determined by using Eqs. (3) and (4). Therefore, the particles begin to move towards the particle with best objective function value, *gbest*.

Step 3: The objective function value is calculated for new positions of each particle. If an agent achieves a better position, the *pbest* value is replaced by the current value. As in Step 1, *gbest* value is selected among *pbest* values. If the new *gbest* value is better than the previous *gbest* value, the *gbest* value is replaced by the current *gbest* value and stored.

Step 4: Steps 1–3 are repeated until the iteration number reaches a predetermined iteration number.

It should be noted that recently Chakraborti et al. [21, 22] have pointed out that PSO is actually a real-coded genetic algorithm, and not a new paradigm. They have also shown how the basic equations in PSO may be dimensionally inaccurate and suggested some better form to be used in the future.

For a single objective problem, the result of the optimization problem will be the position vector of *gbest* at final iteration. The above given PSO procedure is not suitable for solving multiobjective optimization problems, since there is no absolute global minimum (or maximum).

The velocity update step in the PSO is stochastic due to the random numbers generated, which may cause an uncontrolled increase in velocity and, therefore, instability in the search algorithm. In order to prevent this, velocities are limited to the dynamic range of the particle on each dimension. The formulation of the PSO given with Eqs. (3) and (4) corresponds to the global version of the PSO. In addition, a local version of the PSO algorithm also exists. In the local version, particles have information only of their own, and their nearest neighbour best (*lbest*). *gbest* is then replaced by *lbest* in the algorithm.

The algorithm needs more modifications to locate the Pareto front in multiobjective optimization problems. Hu and Eberhart [23] proposed Dynamic neighborhood-particle swarm optimization (DN-PSO) for this purpose. In this approach, instead of defining one global best for the whole population, neighborhoods are defined for each particle, and local *gbest*s are found within these neighborhoods. If a two-dimensional objective function space in a min–min problem is considered, the Pareto front is the boundary of the objective value region, which is the lower left side of the objective function space for min–min problems. The objective of the proposed algorithm is to drop those solutions onto the boundary line indicated by a solid line. For this purpose, the first objective function is fixed to define neighborhoods, and the second objective function is used in optimization. According to the DN-PSO algorithm (1) the distances between the current particle and other particles are calculated in terms of the first objective function, (2) based on these distances, the nearest m (neighbourhood size) particles are found, (3) the local best particle among neighbours is selected in terms of the second objective function. In order to handle constraints, a simple modification to the PSO algorithm is sufficient.

The additional rules that should be implemented in DN-PSO algorithm are: (1) particles should be initiated within feasible region; (2) when updating memories, only the particles within feasible region should be kept in memory. DN-PSO optimization algorithm combined with constraints was converted into a code in Matlab software. This procedure is explained in detail in the previous work [20].

3. Results and discussion

The geometrical features and surfaces are inspected using the imaging system described in Section 2.1. The dimensional and geometrical quality of the grooves produced with the laser milling process exhibit large variations. Table 4 shows some of the grooves produced by using different laser input parameters. These pictures clearly indicate how irregular the laser milling process becomes when grooves with microfeatures are desired to be manufactured. The feedback control which operates on the machine was seen insufficient in order to keep the target width or depth. The effects of input parameters on angles, width, depth, and surface roughness are given with 3-D plots.

Effect of scanning speed and pulse frequency parameters on the surface roughness R_a is presented in Fig. 4, which shows that best surface roughness was obtained at the highest pulse frequency and highest scanning speed combination. The influence of scanning speed on surface roughness in laser micromachining process can be explained as such that laser beam may not affect the surface roughness as much when movement is fast but when movement is slow then surfaces roughness does not improve. However, higher level of pulse intensity improves the surface roughness. Figure 5 shows the effect of pulse frequency and scanning speed on angle geometrical features which is robust and consistent. When scanning speed and pulse intensity is low, the resulting feature angle becomes lower than target feature angle. It is more important to achieve a target feature angle than to obtain trends with the changes in input parameters. For example, it was not possible to achieve target feature angles for A and B when pulse intensity was set to 100% at all. When pulse intensity decreases then there are some cases in which the target feature angle can be obtained. Medium values of scanning speed and pulse frequency are

Table 4.—Test part results pictures.

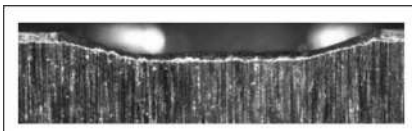	PI = 50% SS = 225 mm/s PF = 80 Hz
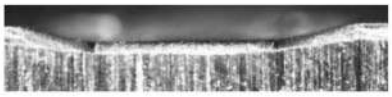	PI = 50% SS = 525 mm/s PF = 60 Hz
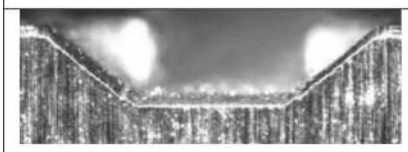	PI = 75% SS = 225 mm/s PF = 80 Hz
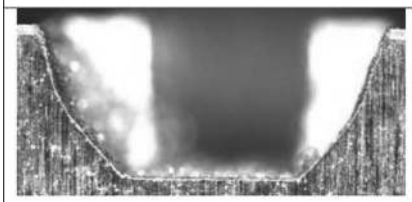	PI = 75% SS = 525 mm/s PF = 60 Hz
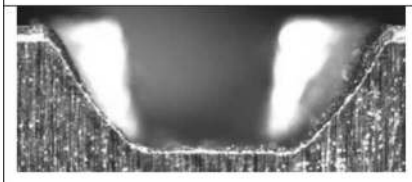	PI = 100% SS = 375 mm/s PF = 100 Hz

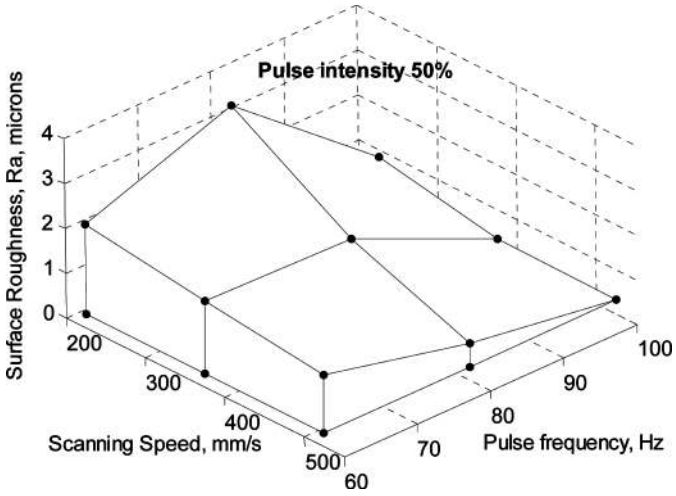

Figure 4.—Effect of pulse frequency and scanning speed on surface roughness.

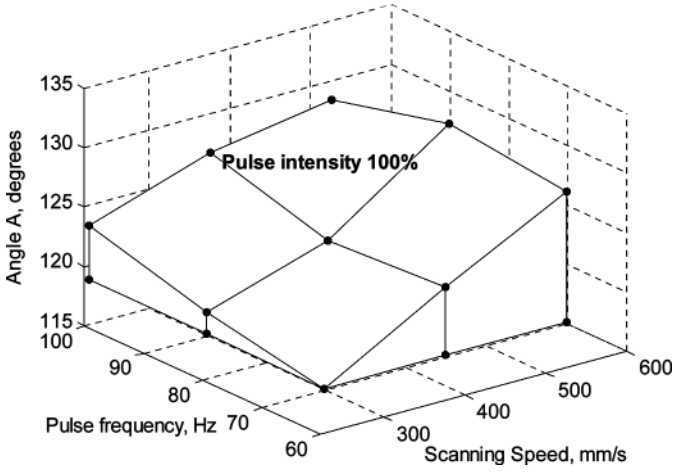

Figure 5.—Effect of pulse frequency and scanning speed on angle geometrical feature.

found to be more appropriate to ensure target feature angles for A and B. When most extreme values of scanning speed and pulse frequency are used, the resultant values of feature angles are the worst.

The effects of scanning speed and pulse frequency on the width feature is different when compared to the feature angles. The target width of 2 mm is achieved at the combination of lowest pulse frequency and highest scanning speed at the 75% pulse intensity (see Fig. 6). All other combinations gave poor results for achieving the width of the groove. Depth feature effects arising from scanning speed and pulse frequency are as expected. Pulse intensity plays an important role in achieving the target depth value. When pulse intensity is lower, it is difficult to obtain the target depth as shown in images in Table 4. When pulse intensity is highest, the groove depth is always larger than the target value of 1 mm. Medium pulse intensity (75%) gives most satisfactory results in groove depth. Combination of higher scanning speed and lower pulse frequency values provide depth values close to the target. Effect of scanning speed and pulse frequency parameters on the volume error ε_{vol} is presented in Fig. 7, which shows that best target volume approximation was obtained at the highest scanning speed and lower pulse frequency values combination. The influence of pulse frequency on volume error in laser micromachining process can be explained as such that laser beam pulses may not affect the volume error as much when those frequency are around lower values. But volume error is affected when high pulse frequency values are considered. However, with scanning speed effects consideration volume error increases when scanning speed gets lower values. Effect of scanning speed on volume error is much significant than pulse frequency. Figure 8 shows the effect of pulse frequency and scanning speed on MRR which is robust and consistent. All combinations of pulse frequency and scanning speed are considered good in order to carry out laser micromachining process but the best option considering productivity rate will be those in which MRR is higher. High MRR is obtained when scanning speed is high and pulse frequency is low. Trends in the figure show how moving pulse frequency from high to low and scanning speed from low to high represents good selections.

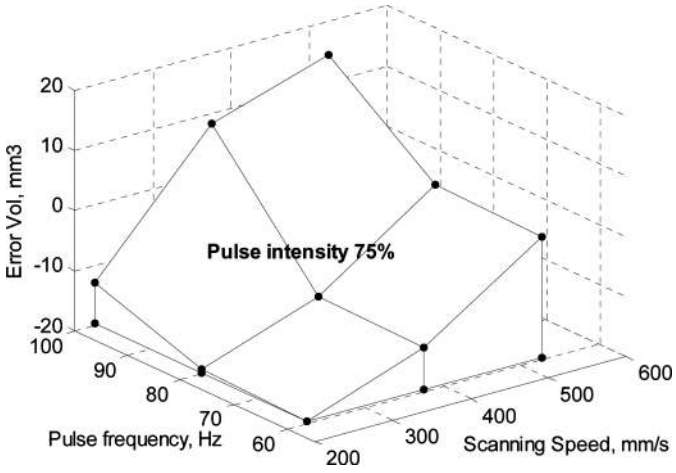

FIGURE 7.—Effect of pulse frequency and scanning speed on error volume.

These figures (Figs. 4–8) illustrate the trends in effects of process parameters on the process outcome; however, these offer no prediction capability, and it is hard to directly utilize the in process planning without using any intelligent computational tool. Therefore, ANNs are employed to capture these complex relations between process inputs and outputs. Selection of optimal process parameters are achieved with PSO by utilizing these neural network models.

3.1. Prediction of Geometrical and Dimensional Features and Surface Roughness Using ANNs

Although the data set presented in Table 2 is not large, it is assumed adequate to train ANNs for modeling the relationships among the laser machining parameters and the geometrical and dimensional features of the

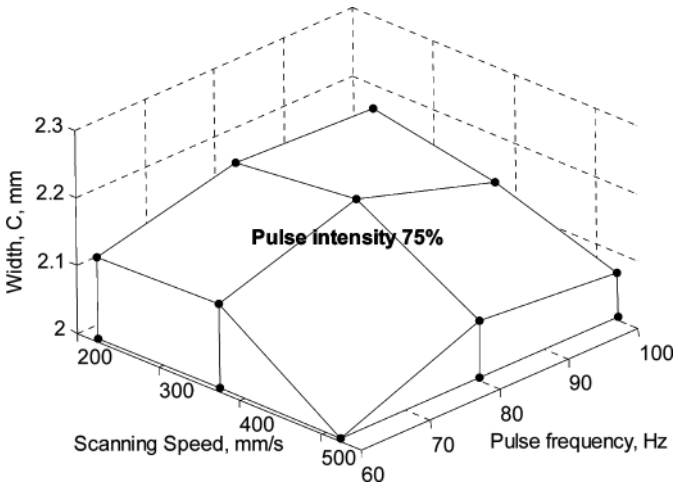

FIGURE 6.—Effect of pulse frequency and scanning speed on width geometrical feature.

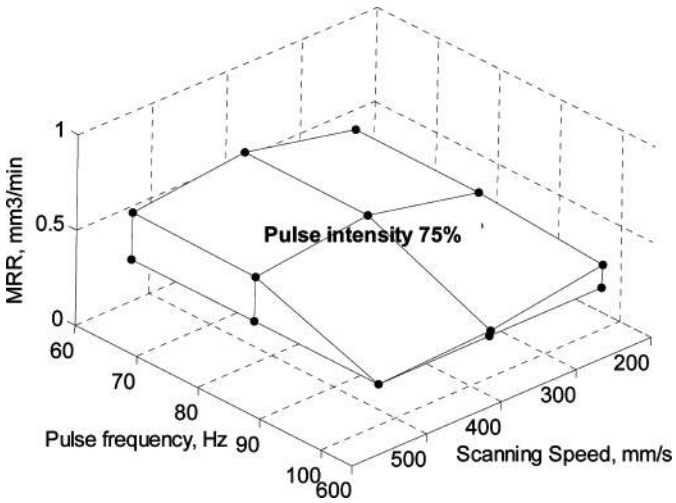

FIGURE 8.—Effect of pulse frequency and scanning speed on MRR.

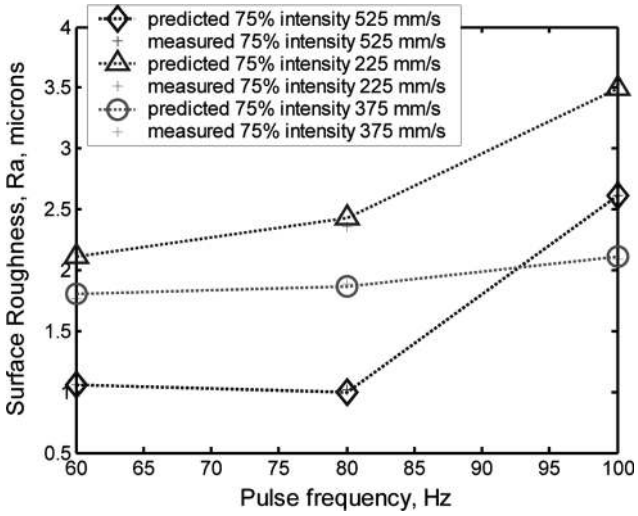

FIGURE 9.—Comparison of surface roughness predictions.

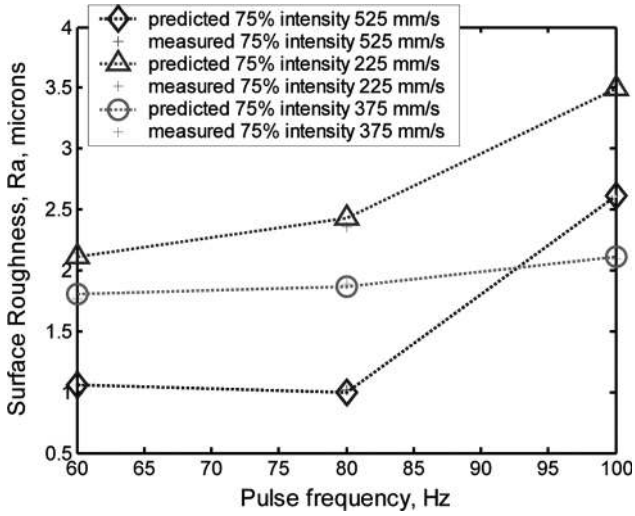

FIGURE 11.—Comparison of predictions for angular feature B.

grooves. Therefore, the experimental data is also utilized in training the ANN as described in Section 2.2. Prediction simulations are arranged with respect to scanning speed and pulse frequency by using trained neural network models. Measured and predicted surface roughness, values of geometrical and dimensional features using the ANN at pulse intensity of 75% and pulse frequency of 60, 80, and 100 Hz are given in Figs. 9–15. These figures indicate the goodness of predictions when neural networks are utilized for selection most optimum laser machining parameters.

3.2. PSO of Laser Micromilling Process Parameters

This work also presents the effects of process parameters on responses such as surface roughness, dimensional and geometrical features, volume error, and MRR. Optimal selection of process parameters of laser micromilling can be formulated and solved as an optimization problem. According to the experiments carried out in this work, laser micromilling operation requires simultaneous consideration of multiple objectives, including achieving minimum surface roughness, minimum error in volume of material removed, and maximum MRR. Usually, process parameters set for one objective function are not suitable for another objective function. This presents a challenge for the optimization problem, since selection of the parameter settings for given multiple choices which may be in conflict to each other. In the laser micromilling process, the optimization problem can be defined as:

$$\begin{aligned} &\min \{f_1(x), f_2(x), f_3(x) \dots\} \\ &\text{s.t.} \quad g_i(x) \le b_i \quad \text{for } i = 1, \dots, m \\ &\qquad g_i(x) = b_i \quad \text{for } i = m+1, \dots, m+k \\ &\qquad x \in X, \end{aligned} \tag{5}$$

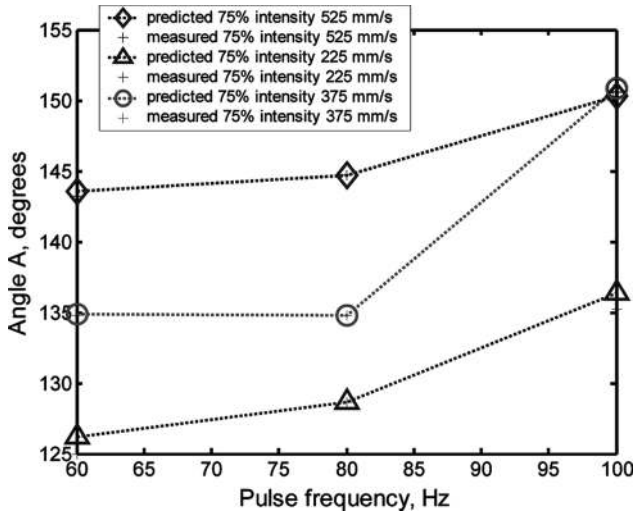

FIGURE 10.—Comparison of predictions for angular feature A.

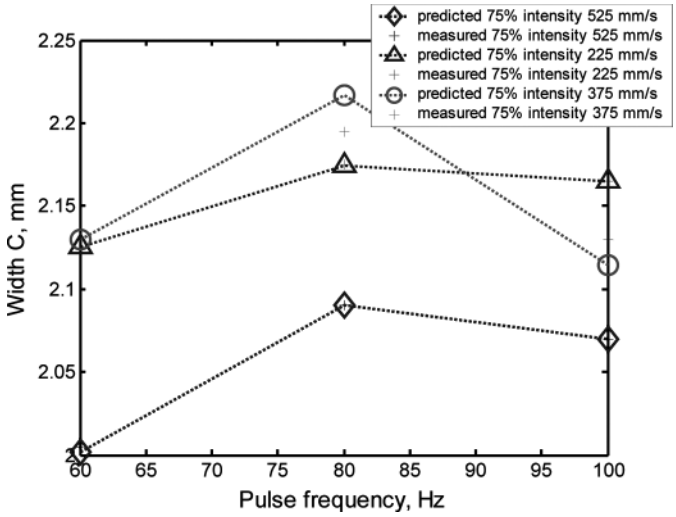

FIGURE 12.—Comparison of width predictions.

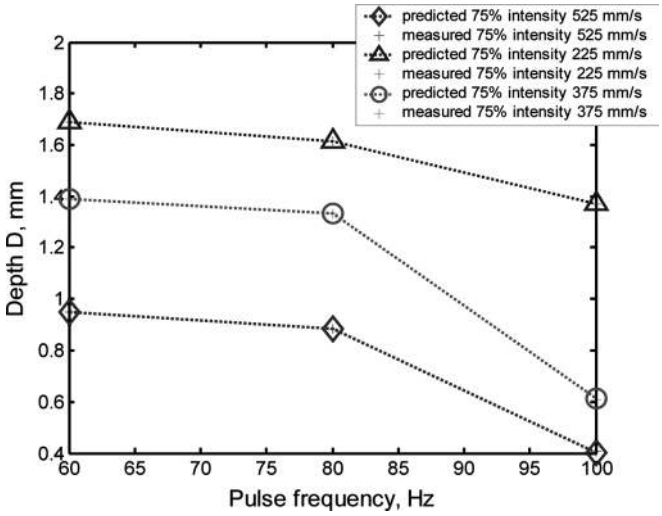

FIGURE 13.—Comparison of depth predictions.

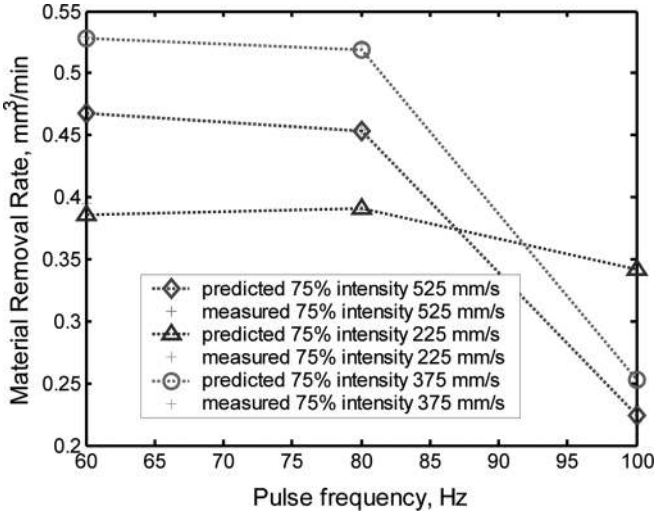

FIGURE 15.—Comparison of MRR predictions.

where

$f_1(x)$ is surface roughness function,

$f_2(x)$ is volume error function,

$f_3(x)$ is MRR function,

...

$g_i(x) = i$th constraint,

$b_i = i$th constraint limit,

x is decision variable vector $(x_1, x_2, \ldots, x_n)$,

x_1 is pulse intensity,

x_2 is scanning speed,

x_3 is pulse frequency.

X is solution space of all possible laser micromachining parameter values, not considering $g_i(x)$ constraints.

In this formulation, the objective is to simultaneously optimize, minimize, or maximize each objective function. The constraints are related to limits of scanning speed and pulse frequency. In solving this optimization problem, there are two general approaches. The first one is based on combining the multiple objectives into single objectives through the use of weights or utility function. The second one is based on Pareto-optimal set of nondominated decision variables settings. The combined objectives approach yields a unique solution that can readily implement, but largely depends on numerical weights that are often difficult to select, and often somewhat selected arbitrarily, in practice. The selection of a Pareto-optimal set avoids this problem,

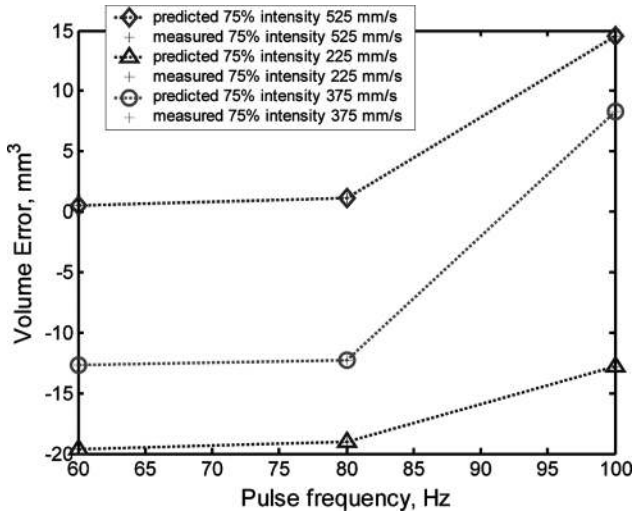

FIGURE 14.—Comparison of volume error predictions.

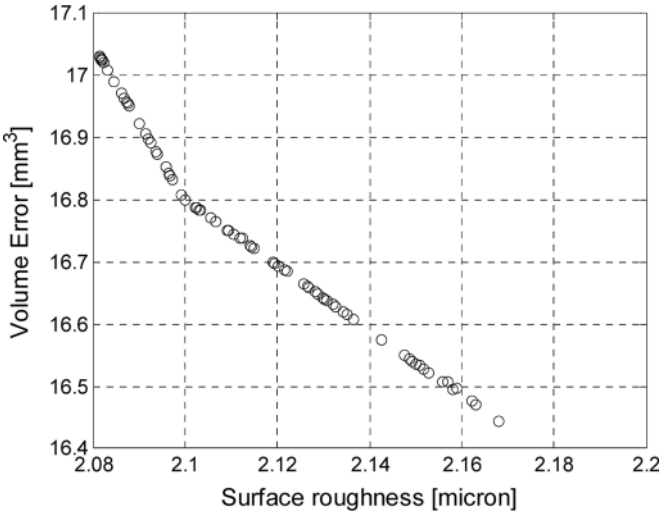

FIGURE 16.—Pareto frontier of optimal laser micromachining parameters.

but may provide numerous prospective solutions that must be considered.

In the case of pulsed laser micromachining process, the following optimization problem can be defined for laser micromachining process with multiple objectives. Decision variables scanning speed *SS*, and pulse frequency *PF*, pulse intensity *PI* are constrained within the ranges of the experiments.

$f_1 =$ minimize (surface roughness),

$f_2 =$ minimize (volume error).

Subject to:

$225\,\text{mm/min} \leq \text{Scan speed} \leq 575\,\text{mm/min}$

$60\,\text{Hz} \leq \text{Pulse frequency} \leq 100\,\text{Hz}$

$50\% \leq \text{Pulse intensity} \leq 100\%.$

The process models are integrated with the PSO to obtain a family of process parameters that satisfies both minimizing surface roughness and minimizing volume error during the selection of laser micromachining parameters. Therefore, Pareto-optimal fronts are computed for representing machining parameters yielding to a certain merit of interest such as MRR, surface roughness, as shown in Fig. 16, that can be selected by the user according to production requirements.

4. Conclusions

In this study, surface finishing and geometrical and dimensional features of the grooves/cavities have been investigated in laser micromachining (laser milling) process of hardened AISI H13 tool steel using pulsed Nd:YAG laser. Multiple linear regression models and neural network models are developed for predicting surface roughness, and geometrical and dimensional features. Predictions of geometrical features and surface roughness with neural network are carried out and compared with experimental data. The results obtained show how neural network models are suitable to predict geometrical features and surface roughness patterns, and can be utilized in process planning for micromachining with Nd:YAG laser technology. In addition an evolutionary computational approach, PSO is applied to the optimizing laser micromachining parameters. The results indicate that the proposed swarm intelligent approach for solving the multiobjective optimization problem with complex objectives is efficient, and can assist the user in process design. Some specific conclusions can be drawn as following:

1. Results obtained in experiments demonstrate large variations in dimensional quality and a need to control laser parameters for precision manufacturing of microgrooves.
2. In the meantime, prediction of geometrical and dimensional quality can be carried out by using ANN which offers good opportunities to select appropriate machining conditions to achieve desired dimensions, angles, and roughness features.
3. Width dimensional feature is difficult to achieve. This feature is in perpendicular direction to the laser beam operation, so as expected the controlling this target is more difficult to carry on.
4. It should be noted that the depth dimensional feature is directly obtained from the same direction of laser beam applied. Therefore, it is highly influenced by the laser pulse intensity, and it is best to use moderate pulse intensity values.
5. Pareto frontier provides a nondominated set of solutions for optimum laser micromachining process parameters.

Acknowledgments

The authors would like to express their gratitude to the ASCAMM Technological Centre for the facilities provided during the experiments and all their valuable support. This work was carried out with the grant supports from the Catalonia Government (project No. 2007 BE 1-0221) and the Spanish Government (project No. DPI 2006-0799).

References

1. Dubey, A.K.; Yadava, V. Laser beam machining—A review. International Journal of Machine Tools and Manufacture **2008**, *48*, 609–628.
2. Pham, D.T.; Dimov, S.S.; Petkov, P.V.; Dobrev, T. Laser milling as a 'rapid' micromanufacturing process. Proceedings of the I MECH E Part B. Journal of Engineering Manufacture **2004**, *218* (1), 1–7.
3. Rajaram, N.; Sheikh-Ahmad, J.; Cheraghi, S.H. CO_2 laser cut quality of 4130 steel. International Journal of Machine Tools and Manufacture **2003**, *43* (4), 351–358.
4. Abdel Ghany, K.; Newishy, M. Cutting of 1.2 mm thick austenitic stainless steel sheet using pulsed and CW Nd: YAG laser. Journal of Materials Processing Technology **2005**, *168* (3), 438–447.
5. Yilbas, B.S. Laser cutting of thick sheet metals: Effects of cutting parameters on kerf size variations. Journal of Materials Processing Technology **2008**, *201* (1–3), 285–290.
6. Thawari, G.; Sarin Sundar, J.K.; Sundararajan, G.; Joshi, S.V. Influence of process parameters during pulsed Nd:YAG laser cutting of nickel-base superalloys. Journal of Materials Processing Technology **2005**, *170* (1–2), 229–239.
7. Bordatchev, E.V.; Nikumb, S.K. An experimental study and statistical analysis of the effect of laser pulse energy on geometric quality during laser precision machining. Machining Science and Technology **2003**, *7* (1), 83–104.
8. Dobrev, T.; Dimov, S.S.; Thomas, A.J. Laser milling: modelling crater and surface formation. Proceedings I Mech E Part C: Journal of Mechanical Engineering **2006**, *220* (6), 1685–1696.
9. Petkov, P.V.; Dimov, S.S.; Minev, R.M.; Pham, D.T. Laser milling: Pulse duration effects on surface integrity. Proceedings of the I MECH E Part B. Journal of Engineering Manufacture **2008**, *222* (1), 35–45.
10. Bandyopadhyaya, S.; Gokhaleb, H.; Sarin Sundar, J.K.; Sundararajanc, G.; Joshi, S.V. A statistical approach to determine process parameter impact in Nd:YAG laser drilling of IN718 and Ti-6Al-4V sheets. Optics and Lasers in Engineering **2005**, *43* (2), 163–182.
11. Li, C.H.; Tsai, M.J.; Yang, C.D. Study of optimal laser parameters for cutting QFN packages by Taguchi's matrix method. Optics and Laser Technology **2007**, *39* (4), 786–795.

12. Quintero, F.; Pou, J.; Lusquiños, F.; Boutinguiza, M.; Soto, R.; Perez-Amor, M. Quantitative evaluation of the quality of the cuts performed on mullite-alumina by Nd:YAG laser. Optics and Lasers in Engineering **2004**, *42* (3), 327–340.
13. Campanelli, S.L.; Ludovico, A.D.; Bonserio, C.; Cavalluzzi, P.; Cinquepalmi, M. Experimental analysis of the laser milling process parameters. Journal of Materials Processing Technology **2007**, *191*, 220–223.
14. Tsai, M.J.; Li, C.H.; Chen, C.C. Optimal laser-cutting parameters for QFN packages by utilizing artificial neural networks and genetic algorithm. Journal of Materials Processing Technology **2008**, *168* (3), 438–447.
15. Yousef, B.F. Neural network modeling and analysis of the material removal process during laser machining. International Journal of Advanced Manufacturing Technology **2003**, *22* (1–2), 41–53.
16. Matlab User's Guide, Neural Network Toolbox, The MathWorks, 2002.
17. Ozel, T.; Karpat, Y. Predictive modeling of surface roughness and tool wear in hard turning using regression and neural networks. International Journal of Machine Tools and Manufacture **2005**, *45* (4–5), 467–479.
18. Ozel, T.; Karpat, Y.; Figueira, L.; Davim, J.P. Modelling of surface finish and tool flank wear in turning of AISI D2 steel with ceramic wiper inserts. Journal of Materials Processing Technology **2007**, *189* (1–3), 192–198.
19. Eberhart, R.C.; Kennedy, J. Particle swarm optimization. Proceedings of IEEE International Conference on Neural Networks, Piscataway, NJ, 1995; 1942–1948.
20. Karpat, Y.; Özel, T. Multi-objective optimization for turning processes using neural network modeling and dynamic-neighborhood particle Swarm optimization. International Journal of Advanced Manufacturing Technology **2007**, *35* (3–4), 234–247.
21. Chakraborti, N.; Jayakanth, R.; Das, S.; Calisir, E.A.; Erkoc, S. Evolutionary and genetic algorithms applied to Li+-C system: Calculations using differential evolution and particle swarm algorithm. Journal of Phase Equilibria and Diffusion **2007**, *28* (2), 140–149.
22. Chakraborti, N.; Das, S.; Jayakanth, R.; Pekoz, R.; Erkoc, S. Genetic algorithms applied to Li^+ ions contained in carbon nanotubes: An investigation using particle swarm optimization and differential evolution along with molecular dynamics. Materials and Manufacturing Processes **2007**, *22* (5–6), 562–569.
23. Hu, X.; Eberhart, R. Multiobjective optimization using dynamic neighborhood particle swarm optimization. Proceeedings of IEEE Swarm Intelligence Symposium 2002; 1404–1411.